

# Thermal Conductivity of Fluids. *n*-Butane

L. T. CARMICHAEL and B. H. SAGE

California Institute of Technology, Pasadena, Calif.

**Measurements of the thermal conductivity of *n*-butane were carried out at pressures up to 5000 p.s.i.a. in the temperature interval between 40° and 340° F. The data were obtained with a spherical conductivity cell and are in reasonable agreement with the data of other investigators obtained with entirely different types of instruments. The results are presented in tabular and graphical form. The residual thermal conductivity appears to be only roughly a single-valued function of specific weight throughout the range of conditions covered in this investigation.**

**E**XPERIMENTAL INFORMATION concerning the thermal conductivity of *n*-butane is limited. Kramer and Comings (5) investigated experimentally the thermal conductivity of *n*-butane at pressures up to 1100 atm. in the temperature interval between 167° and 327° F., and Mann (7), Senftleben (12,13), and Lambert (6) have reported data concerning the thermal conductivity of this hydrocarbon at atmospheric pressure. As a result of limited information concerning the thermal conductivity of *n*-butane and some uncertainty as to the extent to which the residual thermal conductivity can be considered a single-valued function of the specific weight, a systematic investigation of the molecular thermal conductivity of *n*-butane was carried out. These measurements were made at pressures up to 5000 p.s.i.a. in the temperature interval between 40° and 340° F. The thermal conductivity in the critical region was not investigated in detail.

## EQUIPMENT AND METHODS

A spherical conductivity cell was employed in this investigation (8,9,10). This apparatus consists of a gold-plated sphere approximately 3.5 inches in diameter located concentrically within a slightly larger spherical cavity, resulting in a radial transport path of approximately 0.020 inch between the inner sphere and the outer shell. An electrical heater within the inner sphere was so arranged as to yield nearly equal flux at all points around the spherical surface (9). Copper-constantan thermocouples were employed to establish the temperature of the inner spherical surface and the inner surface of the outer shell. It was necessary to make appropriate corrections for the location of the thermocouples within the stainless steel body of the sphere and shell (8). The dimensions of the spherical cavity and the sphere were determined by direct measurement, and the over-all behavior of the instrument was checked by measurements upon the thermal conductivity of helium at atmospheric pressure (2,3,4). At each state measurements were carried out at four different levels of thermal flux. A period of approximately four hours was required to attain steady state at each flux level. Individual corrections for the location of the thermocouples related to the outer surface of the sphere and to the inner surface of the cavity were applied after extrapolation to zero flux (8).

The significant change in the apparent thermal conductivity with flux arises from change in the average temperature of the transport path together with some possible local convection. Gross convection within the spherical transport path was easily detected by rapid increases in the apparent thermal conductivity with an increase in the radial temperature gradient and from a marked disparity between the measurements in the upper and lower hemispheres. Good agreement between measurements in the

upper and lower hemispheres was obtained when gross convection was absent. No indications of gross convection were found except at two states near the critical region.

Measurements of the thermal conductivity of helium were carried out at three different times in the course of the investigation of *n*-butane. These measurements were made at a pressure of approximately 16 p.s.i.a. and at a temperature of 130° F. The three sets of results yielded values from 0.0912 to 0.0914, which are in good agreement with the critically chosen value of 0.0912 B.t.u./(hr.) (ft.)<sup>2</sup>(° F.) reported by Hilsenrath and Touloukian (3). Some difficulty was experienced in completely eliminating the butane from the crevices of the thermal conductivity equipment, and repeated evacuation followed by filling with helium was required to adequately purge the vessel.

## MATERIAL

The *n*-butane employed in this investigation was obtained from the Phillips Petroleum Co. as research grade material with a reported purity of 0.9990 mole fraction *n*-butane. It was found that the vapor pressure of this material at a temperature of 100° F. did not change by more than 0.06 p.s.i. with a change in quality from 0.1 to 0.8. From the results of these measurements, it is believed that the *n*-butane employed did not contain more than 0.0010 mole fraction of material other than *n*-butane. The probable impurities were other hydrocarbons containing four carbon atoms per molecule, predominately isobutane.

## EXPERIMENTAL RESULTS

The influence of thermal flux upon the quantity

$$(q_m/d\theta) / \Delta t_m$$

is shown in the upper part of Figure 1 while the apparent thermal conductivity, with the experimental values individually corrected for the position of the thermocouples, is shown in the lower part of the same diagram. The lines shown in Figure 1 have been fitted by conventional least squares techniques. It is evident that the change in the apparent thermal conductivity with flux is much smaller in the case of *n*-butane than was found for ethane (1). The experimental results were subjected to the analysis described earlier (9). The corrections applied took care of radiant transfer between the spherical surfaces and thermal conduction of the stem supporting the inner sphere. As a result of some small degradation in concentricity of the inner sphere within the cavity amounting to approximately 0.001 inch at 5000 p.s.i., the deviation of the experimental data was slightly larger at the higher pressures. However, it is not believed that this deviation introduced more than 0.10% added uncertainty in the experimental results.

The experimental results are given in Table I. Included are the number of measurements involved for each state, the number of flux levels, the standard error of estimate of the experimentally-measured values from the straight lines, such as are shown in Figure 1, the standard deviation from the area-weighted average of the apparent thermal conductivity at zero flux, and the average change in the apparent thermal conductivity with thermal flux to give an indication of the stability of the system. A total of 45 states were investigated at four different fluxes for almost every situation with a total of approximately 180 observations of the apparent thermal conductivity.

Figure 2 illustrates the influence of temperature upon the thermal conductivity of *n*-butane at atmospheric pressure. The standard error of estimate of the current experimental points from the smooth curve drawn for atmospheric pressure was surprisingly small. The measurements of Kramer (5), Lambert (6), Mann (7), and Senftleben (12, 13) for atmospheric pressure have been included and show a standard error of estimate of 0.00098 B.t.u./ (hr.) (ft.) (° F.) from the smooth curve drawn through the authors' data. The behavior at attenuation was established by extrapolation of the values made at atmospheric pressure to attenuation, based upon the behavior at higher pressures. The analytical expression describing the thermal conductivity at attenuation is:

$$k_0 = A + BT + CT^2 + DT^3$$

The values of the coefficients established from the regression analysis are:  $A = 0.018094$ ,  $B = -0.83530 \times 10^{-4}$ ,  $C = 0.16300 \times 10^{-6}$ , and  $D = 0.70147 \times 10^{-10}$ . The standard error of estimate of the extrapolated values of the present experimental data from this expression was 0.0013 B.t.u./ (hr.) (ft.) (° F.).

In Figure 3 is shown the thermal conductivity of *n*-butane in the gas phase, while similar information for the liquid phase constitutes Figure 4. The standard error of estimate of all of the present experimental data from the smooth curves of these two figures was 0.00028 B.t.u./ (hr.) (ft.) (° F.).

Figure 5 portrays the effect of temperature upon the thermal conductivity of *n*-butane. In the critical region, the behavior has been depicted by dashed lines indicating the existence of significant uncertainty since this region was not studied in detail.

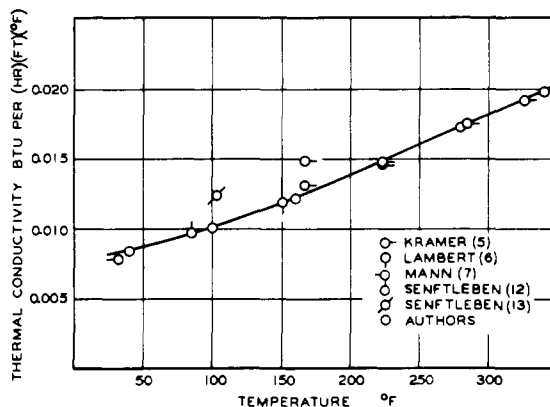


Figure 2. Thermal conductivity of *n*-butane at atmospheric pressure

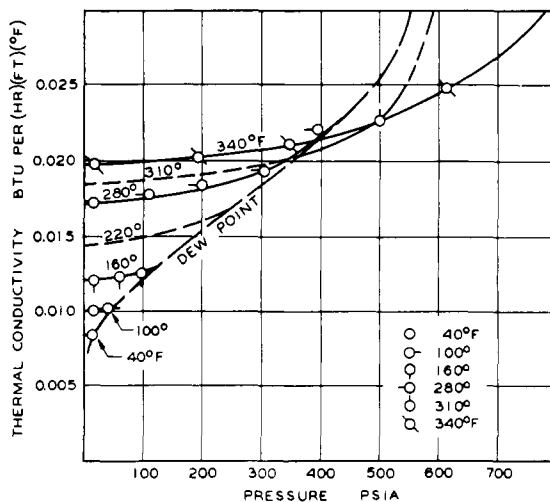


Figure 3. Thermal conductivity of *n*-butane in the gas phase

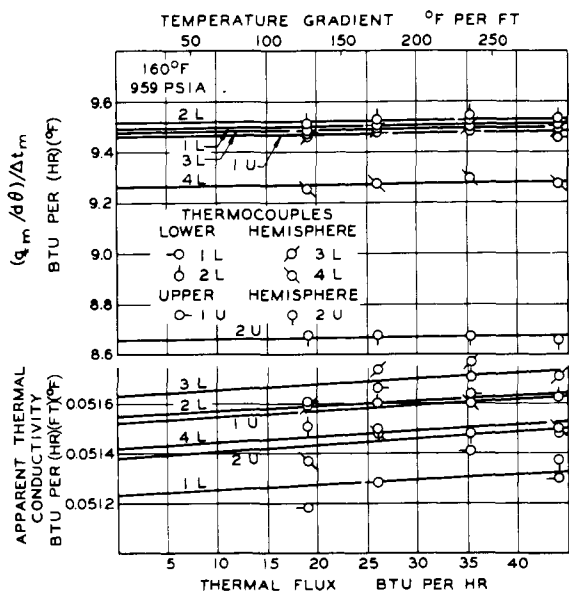


Figure 1. Effect of thermal flux upon apparent thermal conductivity

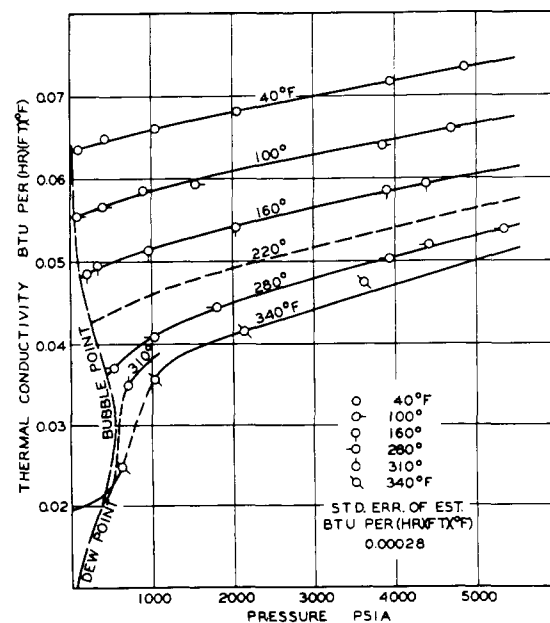


Figure 4. Thermal conductivity of *n*-butane in the liquid phase

Table I. Experimental Conditions

Press., P.S.I.A.	Number Flux Values	Maximum Flux B.t.u./hr.	Number Points	Gradient <sup>a</sup> ° F. <sup>-1</sup>	Standard Error of Estimate <sup>b</sup> (B.t.u./hr.)/(° F.)	Thermal Conductivity B.t.u./ (hr.)(ft.)(° F.)	Standard Deviation <sup>c</sup> B.t.u./ (hr.)(ft.)(° F.)
40° F.							
16	3	13.05	18	0.00484	0.00135	0.008434	0.000060
95	4	57.41	24	0.00120	0.01244	0.063605	0.000362
415	4	56.40	24	-0.00082	0.02428	0.064929	0.000350
1038	4	61.20	24	0.00067	0.03588	0.065999	0.000422
2041	4	61.47	24	-0.00007	0.01004	0.068158	0.000805
3934	4	60.46	24	-0.00068	0.09602	0.071768	0.002065
4849	4	50.72	24	-0.00162	0.01791	0.073505	0.002615
100° F.							
16	4	17.20	24	0.00457	0.00239	0.010040	0.000027
41	3	23.74	18	0.00414	0.00125	0.010266	0.000044
76	4	54.22	24	0.00090	0.01060	0.055457	0.000266
397	4	50.38	24	0.00018	0.01065	0.056693	0.000289
883	4	50.69	24	-0.00230	0.01334	0.058519	0.000529
1539	4	45.90	24	0.00069	0.01198	0.059265	0.000444
3836	4	48.01	24	-0.00033	0.01132	0.064061	0.001740
4683	4	50.71	24	-0.00038	0.00873	0.065992	0.002324
160° F.							
17	4	19.71	24	0.00471	0.00130	0.012043	0.000032
61	4	25.64	24	0.00351	0.00269	0.012274	0.000030
97	4	21.92	24	0.00472	0.00230	0.012329	0.000028
200	4	28.10	24	0.00284	0.01267	0.048573	0.000226
325	4	46.97	24	-0.00033	0.01225	0.049479	0.000178
959	4	44.05	24	0.00037	0.01023	0.051454	0.000119
2038	4	47.60	24	0.00231	0.00100	0.053976	0.000426
3883	4	46.00	24	0.00065	0.00411	0.058523	0.001288
4371	4	47.56	24	0.00010	0.01604	0.059363	0.001322
280° F.							
16	4	23.93	24	0.00347	0.00681	0.017209	0.000131
109	4	23.68	24	0.00465	0.00659	0.017768	0.000252
200	4	23.91	24	0.00291	0.00565	0.018375	0.000249
306	4	22.66	24	0.00356	0.00520	0.019395	0.000222
395	4	24.61	24	-0.00722	0.01689	0.022159	0.000286
522	4	50.60	24	0.01240 <sup>d</sup>	0.04810	0.037123	0.001127
				0.04370 <sup>e</sup>			
1022	4	48.46	24	0.00438	0.01116	0.040994	0.000124
1789	4	44.45	24	0.00171	0.00632	0.044527	0.000219
3928	4	40.98	24	0.00231	0.01434	0.050318	0.000883
4411	2	35.37	12	-0.00237	0.00855	0.051913	0.001226
5321	4	43.20	24	0.00069	0.02100	0.053781	0.001548
310° F.							
395	4	21.81	24	0.00338	0.00385	0.020664	0.000012
501	4	26.48	24	0.01088 <sup>d</sup>	0.00869	0.022611	0.000606
				0.02663 <sup>e</sup>			
694	4	24.00	24	0.02536 <sup>d</sup>	0.04711	0.035001	0.001263
				0.08448 <sup>e</sup>			
340° F.							
17	4	19.95	24	0.00365	0.00340	0.019731	0.000178
192	4	20.89	24	0.00456	0.01071	0.020160	0.000190
347	3	19.38	18	0.00443	0.00442	0.021174	0.000099
614	4	21.58	24	0.01819 <sup>d</sup>	0.01205	0.024872	0.000545
				0.04216 <sup>e</sup>			
1019	4	46.97	24	0.01208 <sup>d</sup>	0.05484	0.035665	0.001265
				0.04364 <sup>e</sup>			
2132	4	50.79	24	0.00605	0.03576	0.041565	0.000226
3611	2	52.10	12	0.00039	0.00537	0.047325	0.000773

<sup>a</sup> Average value of gradient over all thermocouple measurements defined as:  $d[(q_m/d\theta)/\Delta t_m]/d(q_m/d\theta)$ .

<sup>b</sup> Standard error of estimate:  $\sigma = \left[ \left\{ \sum_1^N \left[ \left( \frac{q_m}{\Delta t_m} \right)_e - \left( \frac{q_m}{\Delta t_m} \right)_s \right]^2 \right\} / (N-1) \right]^{1/2}$

<sup>c</sup> Standard deviation from area-weighted average of the six thermocouples:  $s = \left[ \left\{ \sum_1^N (k'_s - k')^2 \right\} / N \right]^{1/2}$

<sup>d</sup> Average value of gradient of lower thermocouples.

<sup>e</sup> Average value of gradient of upper thermocouples.

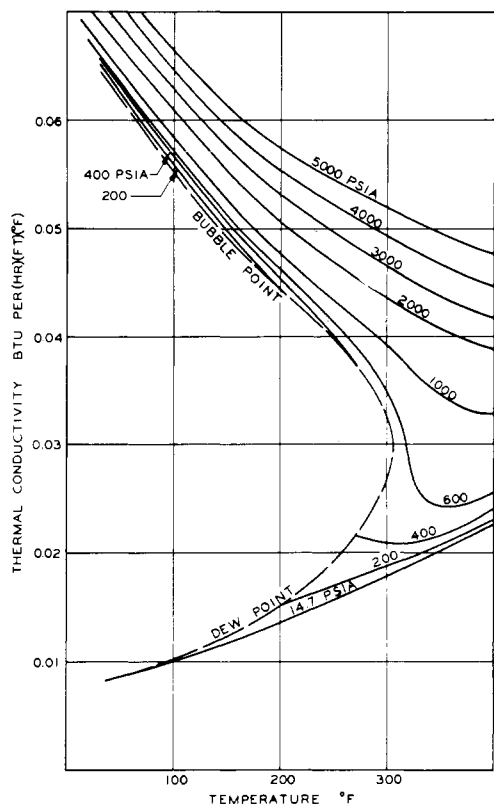


Figure 5. Effect of temperature upon the thermal conductivity of *n*-butane

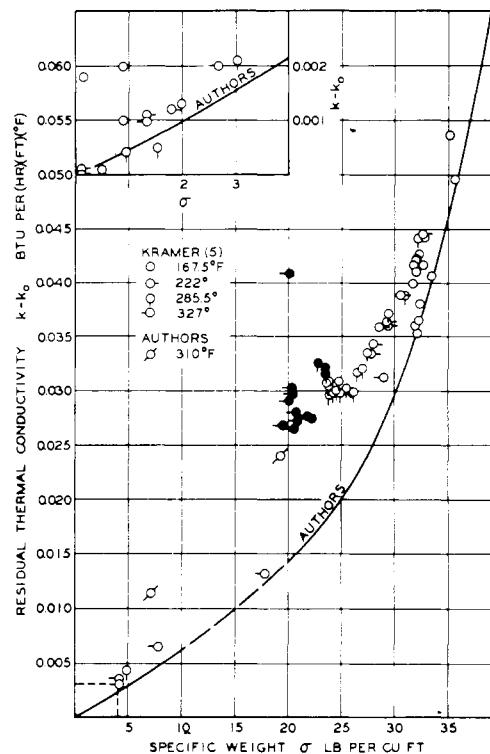


Figure 7. Comparison of measurements from several investigators

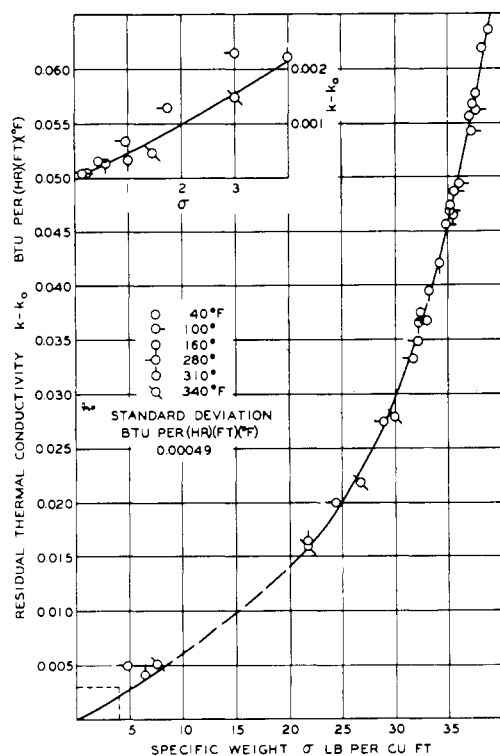


Figure 6. Residual thermal conductivity of *n*-butane

The residual thermal conductivity is shown as a function of the specific weight of *n*-butane in Figure 6. Available experimental data concerning the volumetric behavior of *n*-butane (11) were utilized to establish the specific weight as a function of state. The behavior at low pressures is shown on an enlarged scale in an insert of Figure 6. The curve has been dashed at specific weights between 10 and 20

lb./cu.ft. to denote the absence of experimental measurements in this range of specific weight. The present data, although limited in this range, indicate that the residual thermal conductivity is a single-valued function of specific weight, as was found for ethane (1). However, with consideration of the strong evidence of abnormal behavior reported by Kramer and Comings (5) at 327° F., the single-valued relationship shown by the curve in Figure 6 is still open to question.

Figure 7 presents the residual thermal conductivity as a function of specific weight, including the measurements of Kramer and Comings (5). The full curve is based upon the present measurements shown in Figure 6, and the points wherein Kramer suspected that convection may have caused the difficulty have been indicated in black. The two states investigated by the authors where wide discrepancy between the behavior found in the upper and lower hemispheres was experienced have also been included. It is apparent that these states are in the same general region of temperature and specific weight where Kramer experienced difficulty. Recently Sengers (14) made some measurements upon carbon dioxide near the critical state using a parallel-plate conductivity cell and found a pronounced deviation from the single-valued function of thermal conductivity versus specific weight at temperatures between 77° and 122° F. This effect of carbon dioxide amounts to approximately a seven-fold increase over that which would be predicted for a single-valued curve such as is shown in Figures 6 and 7. Further experimental work will be required in order to establish with certainty the behavior in the critical region of the lighter hydrocarbons. In any event, such behavior is limited to a relatively small region and, as was clearly stated by Kramer (5), it is difficult to ascertain whether the abnormal behavior is a result of local convection or of some anomalous molecular behavior. Since the spherical conductivity cell is not as well suited to investigations in the immediate vicinity of the critical state as some other types of equipment, the matter has not been pursued.

Table II. Thermal Conductivity of *n*-Butane

Press., P.S.I.A.	Temperature, ° F.							
	40	100	160	220 <sup>a</sup>	280	310	340	400 <sup>b</sup>
	(17.66) <sup>c</sup>	(51.5)	(120.6)	(243.2)	(436.0)			
Dew Point	0.00843	0.01011	0.01275	0.01669	0.02275			
Bubble Point	0.06340	0.05531	0.04819	0.04261	0.03609			
14.7	0.00843 <sup>d</sup>	0.01004	0.01204	0.01441	0.01710	0.01839 <sup>e</sup>	0.01973	0.0226
200	0.06389	0.05594	0.04860	0.01605	0.01808	0.01911 <sup>f</sup>	0.02031	0.0232
400	0.06440	0.05669	0.04943	0.04350	0.02127	0.02080	0.02135	0.0240
600	0.06490	0.05737	0.05020	0.04443	0.03782	0.03275	0.02460	0.0255
800	0.06541	0.05797	0.05090	0.04529	0.03965	0.03645	0.03067	0.0298
1000	0.06590	0.05855	0.05155	0.04608	0.04083	0.03818	0.03534	0.0328
1500	0.06702	0.05988	0.05299	0.04761	0.04320		0.03937	0.0371
2000	0.06805	0.06101	0.05424	0.04913	0.04490		0.04120	0.0389
2500	0.06902	0.06203	0.05538	0.05048	0.04643		0.04273	0.0404
3000	0.06999	0.06300	0.05643	0.05170	0.04785		0.04428	0.0418
3500	0.07092	0.06385	0.05749	0.05285	0.04920		0.04580	0.0432
4000	0.07183	0.06470	0.05855	0.05405	0.05050		0.04730	0.0447
4500	0.07270	0.06560	0.05955	0.05515	0.05173		0.04876	0.0463
5000	0.07351	0.06655	0.06050	0.05620	0.05297		0.05015	0.0477
$\sigma$	0.00021	0.00030	0.00017		0.00027	0.00000	0.00046	

<sup>a</sup> Values for this temperature interpolated. <sup>b</sup> Values at this temperature extrapolated from data at lower temperatures. <sup>c</sup> Vapor pressure of *n*-Butane expressed in pounds per square inch. <sup>d</sup> Thermal conductivity expressed in B.t.u./ (hr.) (ft.) (° F.). <sup>e</sup> Interpolated.

<sup>f</sup> Standard error of estimate,  $\sigma$ , expressed in B.t.u./ (hr.) (ft.) (° F.):

$$\sigma = \left[ \frac{\sum_{i=1}^N (k_e - k_s)^2}{(N-1)} \right]^{1/2}$$

Smooth values of the thermal conductivity of *n*-butane in the gaseous and liquid regions are presented in Table II. These data are based upon graphical smoothing operations on large-scale plots similar to the information presented in Figures 3, 4, and 5. The values reported in Table II for the dew-point gas and the bubble-point liquid were obtained by direct extrapolation to vapor pressure. No consideration was given to the abnormalities reported by Sengers (14) and Kramer (5) in the vicinity of the phase boundary.

#### ACKNOWLEDGMENT

This experimental work was carried out through the financial support of the Petroleum Research Fund of the American Chemical Society. H. H. Reamer contributed to the supervision of the experimental work, Joan Jacobs reduced the experimental results, Virginia Berry carried out the necessary calculations to establish the coefficients, and Grace Fitzsimons assisted in the preparation of the manuscript.

#### NOMENCLATURE

*A, B, C, D* = coefficients  
*d* = differential operator  
*k* = thermal conductivity B.t.u./ (hr.) (ft.) (° F.)  
*k*<sub>0</sub> = thermal conductivity at attenuation, B.t.u./ (hr.) (ft.) (° F.)  
*N* = number of points  
*q<sub>m</sub>/dθ* = measured rate of energy addition, B.t.u./hr.  
*s* = standard deviation  
*T* = thermodynamic temperature, ° R.  
 $\Delta t_m$  = measured temperature difference, ° F.  
 $\theta$  = time, hr.  
 $\sigma$  = specific weight, lb./cu.ft.  
 $\sigma$  = standard error of estimate  
 $\Sigma$  = summation operator

#### Superscript

' = uncorrected for pressure effect

#### Subscripts

av. = average  
*e* = experimental  
*s* = smoothed

#### LITERATURE CITED

- (1) Carmichael, L.T., Berry, Virginia, Sage, B.H., J. CHEM. ENG. DATA 8, 281 (1963).
- (2) Hilsenrath, J., et al., "Tables of Thermal Properties of Gases," Natl. Bur. Std. (U.S.), Circ. No. 564 (1955).
- (3) Hilsenrath, J., Touloukian, Y.S., *Trans. Am. Soc. Mech. Engrs.* 76, 967 (1954).
- (4) Keyes, F.G., *Trans. Am. Soc. Mech. Engrs.* 73, 589 (1951).
- (5) Kramer, F.R., Comings, E.W., J. CHEM. ENG. DATA 5, 462 (1960).
- (6) Lambert, J.D., Cotton, K.J., Pailthorpe, M.W., Robinson, A.M., Scrivins, J., Vale, W.R.F., Young, R.M., *Proc. Roy. Soc. (London)* A231, 280 (1955).
- (7) Mann, W.B., Dickens, B.G., *Ibid.*, A134, 77 (1931).
- (8) Richter, G.N., Sage, B.H., *Ind. Eng. Chem., Chem. Eng. Data Ser.* 2, 61 (1957).
- (9) Richter, G.N., Sage, B.H., J. CHEM. ENG. DATA 4, 36 (1959).
- (10) *Ibid.*, 8, 221 (1963).
- (11) Sage, B.H., Lacey, W.N., "Thermodynamic Properties of the Lighter Paraffin Hydrocarbons and Nitrogen," American Petroleum Institute, New York, 1950.
- (12) Senftleben, Hermann, *Z. Angew. Phys.* 5, 33 (1953).
- (13) Senftleben, Hermann, Gladisch, Heinz, *Z. Physik* 125, 653 (1949).
- (14) Sengers, J.V., "Thermal Conductivity Measurements at Elevated Gas Densities Including the Critical Region," Van Gorcum & Company N.V., Assen, The Netherlands, 1962.

RECEIVED for Review February 22, 1964. Accepted June 24, 1964.